Systematic analysis of the expression profiles and prognostic significance of the MED gene family in renal clear cell carcinoma

MIN WANG[1,2], MIN MIN[3], JIA MAI[1,2] and XIAOJUAN LIU[1,2]

[1]Department of Laboratory Medicine, West China Second University Hospital, Sichuan University, Chengdu, Sichuan 610041, P.R. China; [2]Key Laboratory of Birth Defects and Related Diseases of Women and Children (Sichuan University), Ministry of Education, Chengdu, Sichuan 610041, P.R. China; [3]Outpatient Department, The Air Force Hospital of Western Theater, People's Liberation Army, Chengdu, Sichuan 500643, P.R. China

Abstract. The mediator complex (MED) family is a contributing factor in the regulation of transcription and proliferation of cells, and is closely associated with the development of various types of cancer. However, the significance of the expression levels and prognostic value of MED genes in kidney renal clear cell carcinoma (KIRC) have rarely been reported. The present study analyzed the expression and prognostic potential of MED genes in KIRC. The Search Tool for the Retrieval of Interacting Genes/Proteins was used to construct the protein-protein interaction network (PPI), the Assistant for Clinical Bioinformatics database was used to perform correlation analysis, GEPIA 2 was utilized to draw the Kaplan-Meier plot and analyze prognostic significance and the Tumor Immune Estimation Resource was used to assess the association of MED genes with the infiltration of immune cells in patients with KIRC. A total of 30 MED genes were identified, and among these genes, 11 were selected for the creation of a prognostic gene signature based on the results of a LASSO Cox regression analysis. Furthermore, according to univariate and multivariate analyses, MED7, MED16, MED21, MED25 and MED29 may be valuable independent predictive biomarkers for the prognosis of individuals with KIRC. Furthermore, there were significant differences in the expression levels of MED7, MED21 and MED25 in KIRC among different tumor grades. Additionally, patients with KIRC with high transcription levels of MED7, MED21 and MED29 had considerably longer overall survival times. The expression levels of MED genes were also linked to the infiltration of several immune cells. Overall, MED genes may have potential significance in predicting the prognosis of patients with KIRC.

Introduction

Kidney cancer has been one of the top 10 most common types of cancer worldwide for a number of years (1). The incidence of malignant kidney tumors accounts for ~2% of all cancer cases worldwide. Due to various histological and genetic mutations, there are several subtypes of renal cancer, and kidney renal clear cell carcinoma (KIRC) is the most prevalent subtype, accounting for 80% of adult clinical cases worldwide (2,3). The most typical scenario in KIRC is VHL gene mutation or methylation. The tumor suppressor gene VHL encoded by chromosomal arm 3p is widely lost in KIRC (4,5). Patients with VHL mutations have a greater lifetime risk of recurrent cancer, along with an increased risk of tumor development in several organs (2). Notably, to the best of our knowledge, no genetic biomarker has been identified as a viable predictor of KIRC prognosis or treatment outcome; therefore, efforts should be made to develop effective biomarkers.

The mediator complex (MED) gene family forms a multiprotein complex that connects transcription factors to RNA polymerase II, which extensively participates in the proliferation, differentiation and migration of cells (6). Notably, the MED is a protein complex that has evolved to mediate specific protein-protein interactions (PPIs) (7). The MED is evolutionarily conserved and has a similar structure in both yeast and humans, containing a head, middle, tail and kinase module (8). In general, the MED is considered to be a transcriptional coactivator; however, it was previously identified as a genetic suppressor of the Ras/MAP kinase pathway (9). Mediator subunits serve a role in cellular signaling pathways, including EGFR signaling, Wnt signaling and ERK/MAPK signaling (10). Furthermore, as a highly conserved member of the MED family, MED21 can affect PPARA-related gene expression and metabolism (11). In addition, loss of MED7 has been demonstrated to have a substantial impact on numerous aspects of cellular function, including metabolism (12).

Correspondence to: Dr Jia Mai or Dr Xiaojuan Liu, Department of Laboratory Medicine, West China Second University Hospital, Sichuan University, 20, Section 3, Ren Min Nan Lu, Chengdu, Sichuan 610041, P.R. China
E-mail: maijia@mail2.sysu.edu.cn
E-mail: xiaojuanliu1979@163.com

Notably, there is a strong relationship between the MED family and cancer biology; for example, a mechanistic investigation indicated that MED19 is highly expressed in breast cancer tissues, and is significantly related to larger tumors, high-grade malignant characteristics and poor prognosis (13). Another study also showed that most uterine leiomyomas have mutations in MED12 exon 2 (14). Furthermore, it has been revealed that MED19 disruption prevents tongue cancer cells from proliferating and migrating (15). In addition, MED7 has been linked to improved long-term survival outcomes and favorable prognostic traits in patients with breast cancer, and its expression is increased in hepatocellular carcinoma (HCC) and is related to the progression of HCC (16,17). Moreover, high MED21 expression levels are associated with poor HCC prognosis, according to a comprehensive analysis (18). The nuclear transcription-related protein NF-κB is involved in cell adhesion, proliferation and differentiation, and is often active in tumor cells; according to a previous study, transcription of a reporter gene (firefly luciferase) controlled by NF-κB can be inhibited by MED21 RNA interference (RNAi) (19).

Although a number of research studies have been conducted to investigate the underlying mechanisms involved in various malignancies, to the best of our knowledge, no investigations have focused on the therapeutic and prognostic value of the MED family in patients with KIRC or other types of kidney cancer. Therefore, the present study aimed to analyze the expression and prognostic significance of MED in KIRC. The present study used bioinformatics to examine the predictive value of the MED gene family in KIRC and created a risk score based on public databases. The present findings may offer novel insights into selecting MED genes as appropriate prognostic biomarkers in KIRC.

Materials and methods

Data acquisition and analysis. mRNA expression data and relevant clinical information of 532 patients were collected from The Cancer Genome Atlas (TCGA)-KIRC dataset (https://portal.gdc.cancer.gov/), and the acquisition and application methodology followed the corresponding guidelines and policies. R (version 4.0.3) software (https://www.r-project.org/) and R Bioconductor packages (http://bioconductor.org/) were utilized to examine the data. There were no ethical concerns because these data were available online. Additionally, not all of the information, such as overall survival data, was available for all of the data parameters.

Construction of the PPI. The MED is a protein complex that has evolved to mediate specific PPIs (7). PPI network analysis was used to examine the potential interactions between the MED genes. The Search Tool for the Retrieval of Interacting Genes/Proteins (version 11.5) (https://cn.stringdb.org/) was used to construct a PPI network. A total of 30 MED genes were entered into the search box. The active interaction sources selected included text mining, experiments, databases, co-expression, neighborhood, gene fusion and co-occurrence; the minimal needed interaction score was set at 0.4.

Correlation analysis. For TCGA-KIRC cohort, RNA-sequencing expression profiles and associated clinical data were obtained from TCGA dataset. The R software package ggstatsplot (https://indrajeetpatil.github.io/ggstatsplot/) was used to construct a two-gene correlation map. The correlation between quantitative variables was assessed using Spearman's correlation analysis for non-normally distributed data. P<0.05 was considered to indicate a statistically significant difference, and correlation coefficients >0.3 were considered to indicate a correlation. The website Assistant for Clinical Bioinformatics (https://www.aclbi.com/static/index.html#/), which integrates all of these features, was used for these analyses.

Functional and pathway enrichment analyses. Using the clusterProfiler R package (https://www.bioconductor.org/packages/release/bioc/html/clusterProfiler.html), Gene Ontology (GO) analysis was carried out to determine the putative biological roles of the 30 MED genes. Thresholds of P<0.05 and q<1 were set for the GO enrichment analyses.

Identification of molecular subtypes. All of these analyses were carried out using the web application Assistant for Clinical Bioinformatics (https://www.aclbi.com/static/index.html#/). TCGA data were used to obtain raw RNA-sequencing data and related clinical data, and a cluster analysis of 30 MED genes in 532 patients with KIRC was performed. In addition, ConsensusClusterPlus (version 1.60.0) was used for consistency analysis. The number of clusters was limited to six, and 80% of the entire sample was analyzed 100 times. Clustering heatmaps were created using the Pheatmap package (version 1.0.12). The survival ROC program was used to construct survival curves after analyzing prognostic differences among distinct subgroups (groups C1, C2 and C3).

Construction of the risk assessment model. All these analyses were performed using the web tool called ASSISTANT for Clinical Bioinformatics that combines all these functions (https://www.aclbi.com/static/index.html#/). The logistic LASSO model is a shrinkage technique that positively chooses variables from a sizable and potentially multicollinear set in the regression, producing a set of predictors that is pertinent and understandable. Using LASSO regression analysis, a predictive signature was created that divided 532 patients into high-risk and low-risk groups by calculating the customized risk score with coefficients, and the cut-off value was the median risk score. Kaplan-Meier survival analysis with log-rank test was then performed to analyze the differences in survival between the aforementioned two groups. Additionally, to compare the prediction accuracy of each gene and risk score, a TimeROC (v 0.4) analysis was performed.

Survival prognostic analysis. The overall survival (OS) data for MED genes in TCGA-KIRC cohort were obtained and processed using GEPIA 2 (http://gepia2.cancer-pku.cn/). The expression thresholds, cut-off high (50%) and cut-ff low (50%), were used to divide 532 patients into high- and low-expression cohorts, respectively. The log-rank test was used to analyze the OS data. P<0.05 was considered to indicate a statistically significant difference.

Establishment of a five-gene-based prognostic gene signature. Univariate and multivariate analyses were performed using

Table I. siRNA sequences against human MED7 and MED21 genes.

siRNA	Sense, 5'-3'	Antisense, 5'-3'
MED7-siRNA1	CAAGGAAUAUACGGAUGAA(dT)(dT)	UUCAUCCGUAUAUUCCUUG(dT)(dT)
MED7-siRNA2	CCUGGAACGAGUAAUUGAA(dT)(dT)	UUCAAUUACUCGUUCCAGG(dT)(dT)
MED21-siRNA1	CAGGCUGCUAGCUUGUAUA(dT)(dT)	UAUACAAGCUAGCAGCCUG(dT)(dT)
MED21-siRNA2	GGAGGAUGUUGUUUAUCGA(dT)(dT)	UCGAUAAACAACAUCCUCC(dT)(dT)
siRNA-UNC	UUCUCCGAACGUGUCACGU(dT)(dT)	ACGUGACACGUUCGGAGAA(dT)(dT)

MED, mediator complex; UNC, universal negative control; siRNA, small interfering RNA.

the Cox regression model approach. These analyses can assess whether the predictive gene signature could be a factor that does not depend on other pathological or clinical factors, such as age, sex, pathological tumor-node-metastasis (TNM) stage, and tumor grade. $P<0.05$ was considered to indicate a statistically significant difference. All independent prognostic factors identified by multivariate Cox regression analysis were used to construct a nomogram to explore the likelihood of 1-, 2-, 3- and 5-year OS in patients with KIRC. All of these analyses were carried out using the Assistant for Clinical Bioinformatics web tool.

Immune infiltration analysis. The Tumor Immune Estimation Resource (TIMER; http://timer.cistrome.org/) was used to investigate the relationships between MED7, MED16, MED21, MED25 and MED29 expression, and immune infiltration across TCGA-KIRC cohort. CD8^{+} T cells, CD4^{+} T cells, B cells and macrophages were chosen as the immune cells for analysis. The TIMER method was used to estimate immunological infiltration. The purity-adjusted Spearman's rank correlation test was used to generate the estimated P-value to assess the relationships between MED genes and invading immune cells.

Immunohistochemistry (IHC) analysis. KIRC tissues and paired adjacent normal tissues from 10 patients (age, 37-77 years) were used for the IHC analysis. KIRC tissue chips (cat. no. HKidE020PG01) fixed in 4% paraformaldehyde at room temperature for 48 h and embedded in paraffin were purchased from Shanghai Xinchao Biological Technology Co., Ltd. The tissue chips were successively placed in xylene for 10 min, absolute ethanol for 5 min and 75% alcohol for 5 min, and washed with pure water. The tissue sections were placed in Tris-EDTA antigen repair buffer (pH 9) in a microwave oven for antigen repair. The solution was heated at medium heat for 8 min and kept warm for 8 min before being transferred to medium and low heat for 7 min. After natural cooling, the glass slides were placed in PBS (pH 7.2-7.4) and washed on a decolorization shaker three times for 5 min each, followed by incubation with 0.1% Triton X-100 at room temperature for 10 min for permeabilization. The glass slides were placed in PBS (pH 7.2-7.4) and washed on a decolorization shaker three times for 5 min each. A total of 50 μl 5-10% normal goat serum (cat. no. ab7481; Abcam) was added per chip for blocking (1:19 fold dilution) at room temperature for 30 min. Immunohistochemical staining of the paraffin-embedded

tumor tissues was performed using primary antibodies against MED7 (1;200; cat. no. K107987P; Beijing Solarbio Science & Technology Co., Ltd.) and MED21 (1;200; cat. no. K107312P; Beijing Solarbio Science & Technology Co., Ltd.) at 4˚C overnight, HRP-conjugated goat anti-rabbit secondary antibodies (1:200; cat. no. GB23303; Wuhan Servicebio Technology Co., Ltd.) at room temperature for 1 h, and an ABC Elite immunoperoxidase kit (Wuhan Servicebio Technology Co., Ltd.) according to the manufacturer's instructions. Subsequently, an optical microscope was used to examine all visible fields, and the particles in the cell cytoplasm that were stained brown were considered positive. IHC analysis of human samples was approved by the Institutional Review Board of West China Second University Hospital (ethics approval no. 2023-012; Chengdu, China). All procedures complied with the applicable norms and regulations.

Cell culture and reagents. The 786-o cells (human clear cell adenocarcinoma cells) were purchased from Procell Life Science & Technology Co., Ltd., and were maintained in RPMI 1640 (Gibco; Thermo Fisher Scientific, Inc.) supplemented with 10% FBS (Nanjing SenBeiJia Biological Technology Co., Ltd.) at 37˚C in an incubator containing 5% CO_2.

Small interfering RNA (siRNA) transfection and transfection efficiency verification. The corresponding siRNAs were designed to disrupt the gene expression of MED7 and MED21 (Table I). Briefly, 786-o tumor cells ($6x10^5$ per well) were seeded in 6-well plates the day before, and when the cell density reached 80% on the 2nd day, 100 pmol siRNA and Lipofectamine® 2000 (cat. no. 100014469; Invitrogen; Thermo Fisher Scientific, Inc.) mixture was added according to the standard protocol. The culture medium was changed after 6 h, and the plates were incubated at 37˚C in an incubator containing 5% CO2. After 48 h, other assays were performed and TRIzol® (cat. no. 15596018CN; Invitrogen; Thermo Fisher Scientific, Inc.) was used to extract the RNA. Subsequently, the Evo M-MLV RT Mix Kit (cat. no. AG11728; Accurate Biology) was used to perform reverse transcription PCR (RT-PCR) according to the manufacturer's protocol, and then SsoFast™ EvaGreen® Supermix (cat. no. 1725200; Bio-Rad Laboratories, Inc.) was used to perform quantitative PCR (qPCR) according to the manufacturer's instructions. The thermocycling conditions were as follows: Pre-denaturation at 95˚C for 5 min, followed by 40 cycles of denaturation at 95˚C for 10 sec, annealing at 60˚C for 30 sec and extension
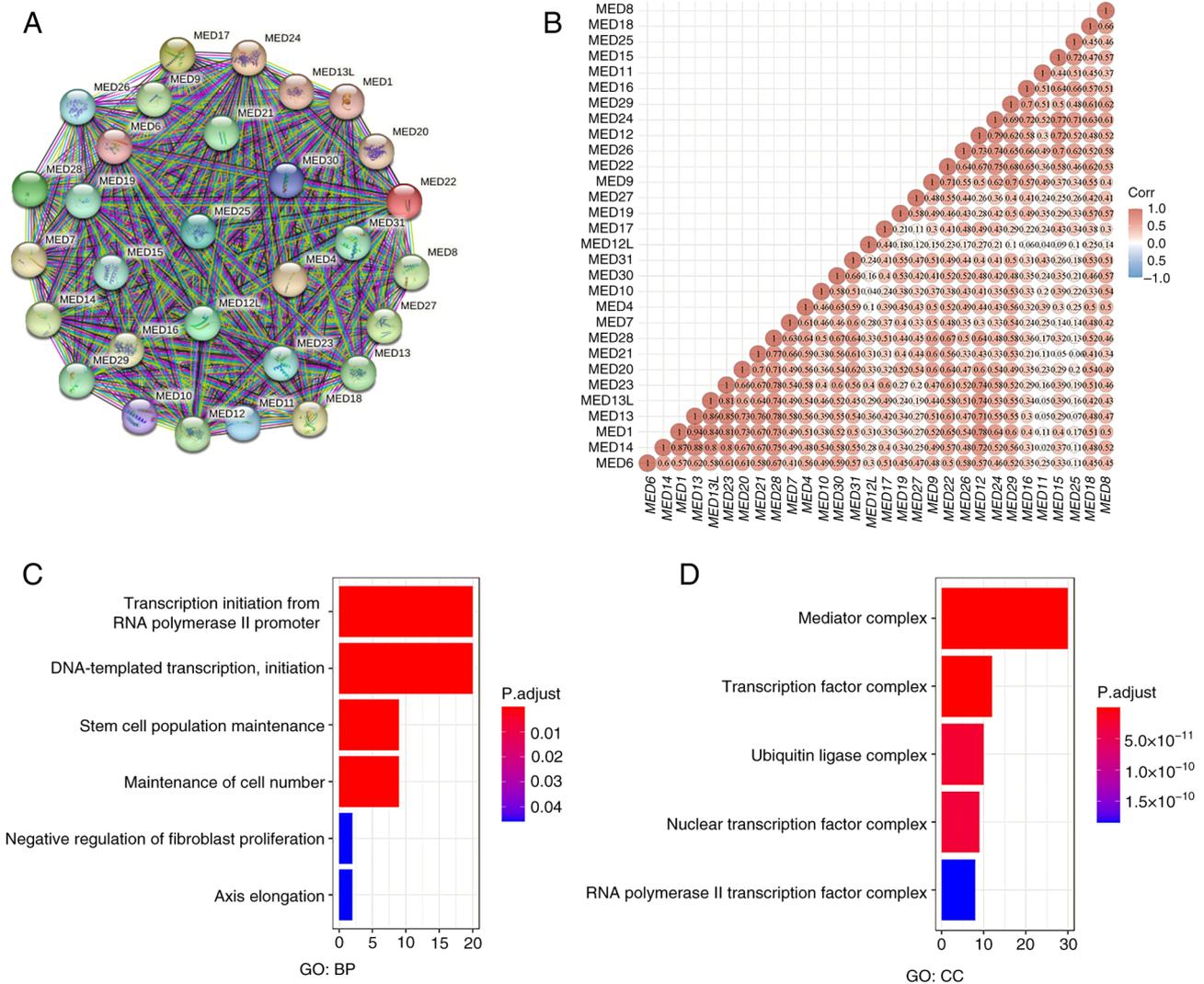
Figure 1. Correlation analysis of the MED gene family, and its associated pathways and molecular functions. (A) Protein-protein interaction network of the MED gene family. (B) Correlations between 30 MED genes with each other. (C) GO BPs of the MED gene family. (D) GO CCs of the MED gene family. BP, biological process; CC, cellular component; GO, Gene Ontology; MED, mediator complex.

at 60˚C for 30 sec. The results were analyzed using the $2^{-\Delta\Delta Cq}$ method to verify the transfection efficiency (20). The primer sequences were as follows: MED7, forward 5'-TATTCAAGA AGGCTTAGCTCCC-3', reverse 5'-TCATCACATTGGAAC TGATTGC-3'; MED21, forward 5'-GCAGATCAGTTTTGT AATGCCA-3', reverse 5'-AAGCAGCTGTAGATTCTTCAC T-3'; GAPDH, forward 5'-TGCACCACCAACTGCTTAGC-3' and reverse 5'-GGCATGGACTGTGGTCATGAG-3'.

Transwell assay. For the migration assay, 24-well Transwell inserts (pore size, 8 μm; cat. no. 11310; BeiJing LABSELECT;) were used. To the upper chamber of the Transwell inserts, 786-o tumor cells (1x10⁵) were plated in 200 μl FBS-free culture medium. To the lower chamber, 600 μl culture medium containing 10% FBS was added as a chemoattractant. After 48 h of culture in a 37˚C incubator, the cells that had migrated the lower surface of the filters were fixed in 4% formaldehyde at room temperature for 10 min and stained with 0.1% crystal violet solution at room temperature for 10 min, and observed under a light microscope.

Wound healing assay. Briefly, 786-o tumor cells (6x10⁵ cells per well) were seeded in 6-well plates the day before, and the culture medium was supplemented with 2% FBS. When the cell confluence reached nearly 100%, a wound was created by manually scraping the cell monolayer with a 200-μl pipette tip. A light microscope camera was used to visualize the changes in the wound at 0 and 24 h.

Statistical analysis. R version 4.0.3 was used for statistical analysis. The Kaplan-Meier method was used to plot survival curves. Log-rank tests, and multivariate and univariate Cox proportional hazards regression analysis were used to generate P-values and hazard ratios (HRs) with 95% confidence interval (CI) values for Kaplan-Meier curves. Unpaired two-tailed Student's t-test was used to analyze the data between two groups, and one-way ANOVA was used to analyze the data among three or more groups, and Dunnett's test was used as the post hoc multiple comparisons test. In addition, Shapiro-Wilk test was used to assess data normality. Assays were repeated three times.
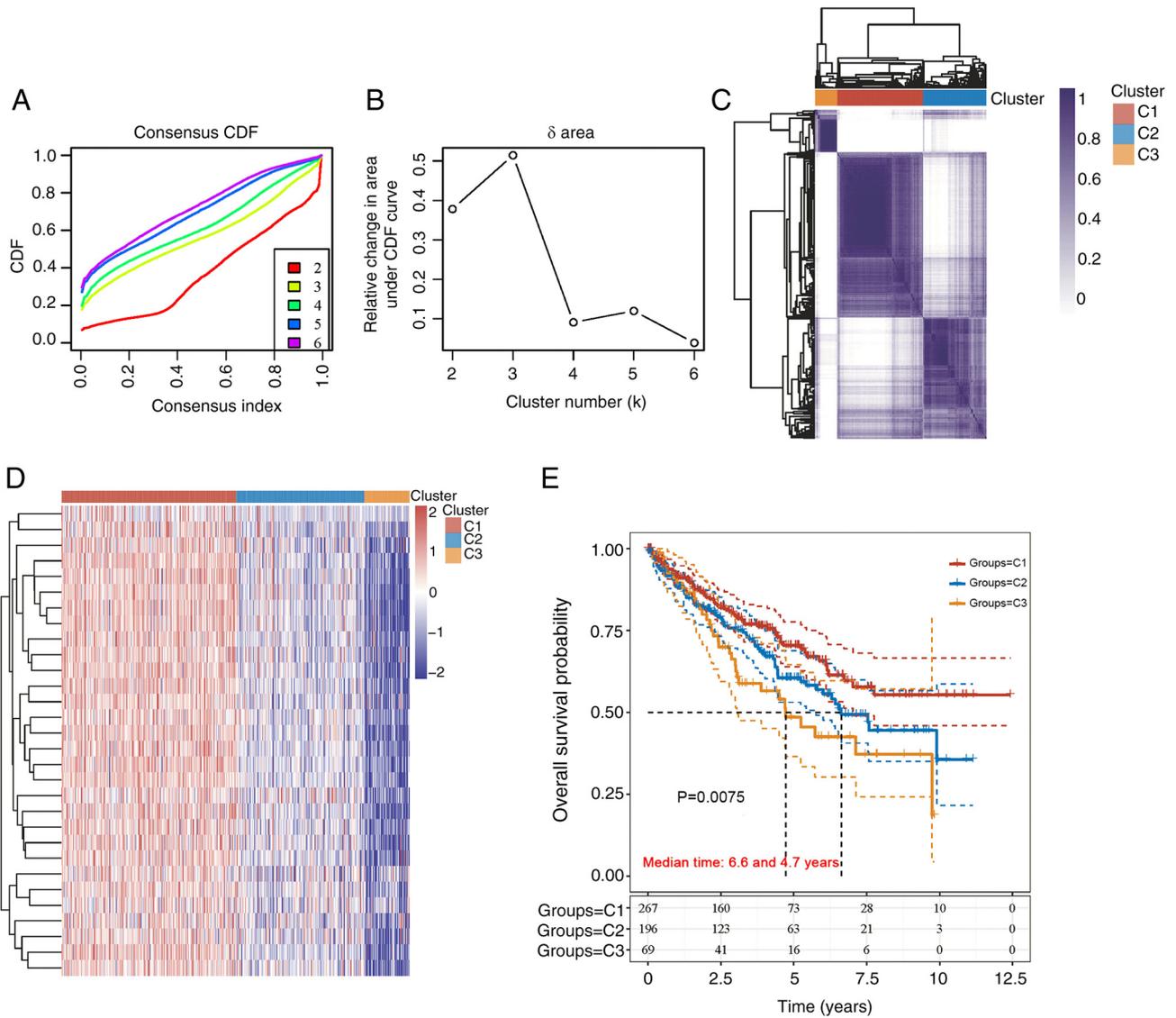
Figure 2. Patients with kidney renal clear cell carcinoma were divided into different molecular types in accordance with the MED gene family. (A) CDF curve. Different clusters are distinguished by different colors. (B) Consensus clustering based on δ area curve. (C) Heatmap of sample clustering at consensus k=3. (D) Gene expression heatmap of significant prognostic genes in C1, C2 and C3 subtypes. The gene expression level varies from -2 to 2, with red denoting high expression and blue denoting low expression. (E) Survival curves of different cluster groups. CDF, cumulative distribution function; MED, mediator complex.

P<0.05 was considered to indicate a statistically significant difference.

Results

Relationships within the MED gene family. According to the PPI analysis results, the details were as follows: Number of nodes, 30; number of edges, 435; mean node degree, 29; PPI enrichment, $P<1.0 \times 10^{-16}$. These numbers suggested that the MED family genes interacted strongly (Fig. 1A). Additionally, the relationships between MED family genes were determined by examining their mRNA expression in KIRC with the R software package ggstatsplot, which included Spearman's correlation analysis. The findings revealed substantial correlations between genes, such as between MED1 and MED13, between MED14 and MED13, and between MED13L and MED23 (Fig. 1B). Functional enrichment analysis revealed that 'transcription initiation from RNA polymerase II promoter', 'DNA-templated

transcription, initiation', 'stem cell population maintenance' and 'maintenance of cell number' were significantly related to MED family genes (Fig. 1C). Additionally, 'mediator complex' and 'transcription factor complex' were the most common cellular components (Fig. 1D).

Molecular subtype of KIRC based on MED family genes. The unsupervised clustering of 532 samples from patients with KIRC for MED family genes was carried out using ConsensusClusterPlus software. The maximum number of clusters was six (Fig. 2A), and the cumulative distribution function curve of the MED family genes revealed that k=3 was a good candidate for clustering (Fig. 2B). In addition, the heatmap of the clustering results displayed in Fig. 2C demonstrated a relatively consistent distribution of samples in the three clusters (C1, C2 and C3). As a result, patients with KIRC were classified into C1, C2 and C3 subtypes. To examine the expression of MED genes in the three subtypes, a heatmap
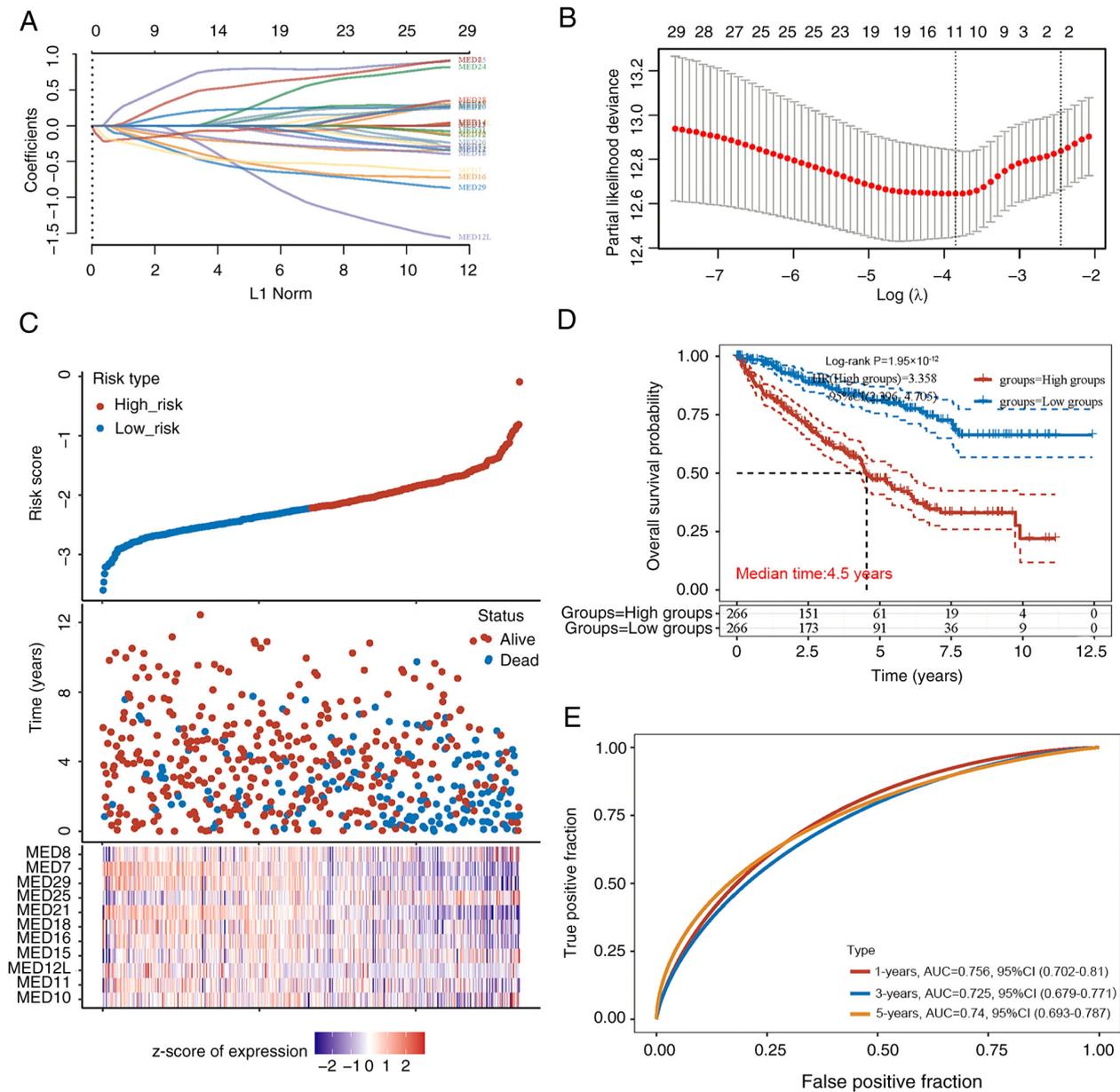
Figure 3. Construction and validation of an 11-gene signature in patients with kidney renal clear cell carcinoma. (A) Altering trajectory of different independent variables. To find the hub genes, the least absolute shrinkage and selection operator regression methods were applied. (B) Confidence interval under each λ. (C) Distribution of risk scores, summary of survival, and heatmap of the 11 genes in the high-risk group and low-risk group. (D) Survival curve distribution of the 11-gene signature in the two groups (P=1.95x10^{-12}). (E) Time-dependent receiver operating characteristic curve for 1-, 3- and 5-year survival prediction. AUC, area under the curve; MED, mediator complex.

was created (Fig. 2D). Survival analysis revealed a significant difference among the C1 (n=267), C2 (n=196) and C3 (n=69) subtypes. Compared with those in the C2 and C3 subtypes, the prognosis of patients in the C1 subtype was better (Fig. 2E).

Construction and validation of an 11-gene signature in patients with KIRC. The most important prognostic genes within the MED family were identified using the LASSO regression technique. According to the independent variable change trajectory, there were more independent variable coefficients with a tendency to zero as λ steadily decreased. When variable coefficients reached zero, it meant these variables contributed little to the model at this point, and they can be excluded in the model (Fig. 3A). Based on this, the 10-fold cross-validation

approach was used to create a risk model and the CI under each λ was examined (Fig. 3B). The risk model included 11 MED genes, and the details of the formula used were as follows: Risk score=(0.2023) x MED10 + (-0.1896) x MED11 + (-0.2343) x MED12L + (0.0053) x MED15 + (-0.38) x MED16 + (-0.1433) x MED18 + (-0.0739) x MED21 + (0.7374) x MED25 + (-0.4641) x MED29 + (-0.4498) x MED7 + (0.4838) x MED8. The risk score of each patient with KIRC was calculated, and based on the median risk score (cut-off value, -2.2), the patients were divided into two groups: Low-risk (n=266) and high-risk (n=266). The distribution of the 11 genes in all the samples showed that patients in the high-risk group had higher levels of MED25 expression. The individuals in the low-risk group, however, were more likely to express MED7 and MED21
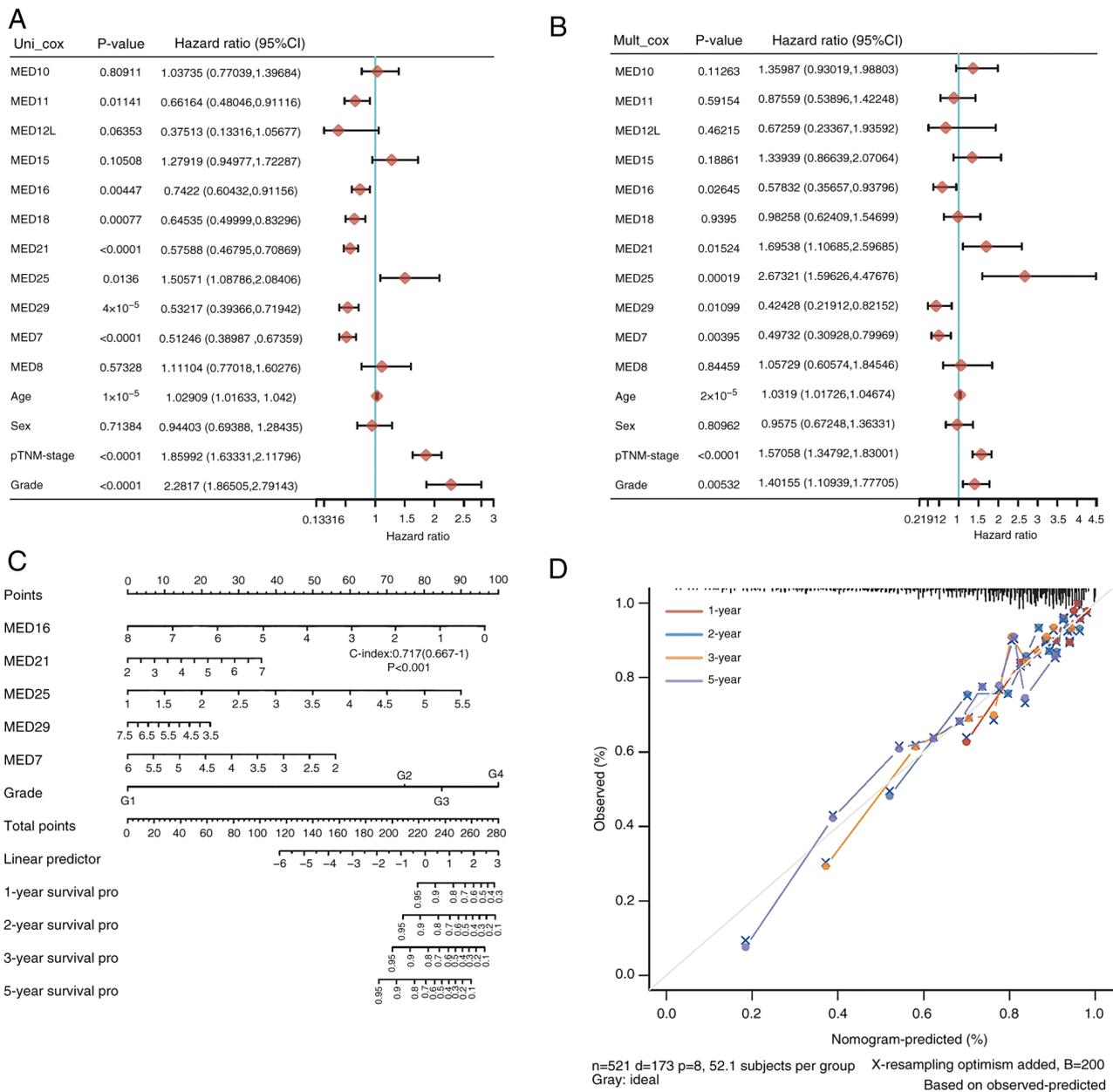
Figure 4. Clinical prognostic value of a five-gene signature in patients KIRC. (A) Univariate and (B) multivariate Cox analyses of the MED family genes in TCGA-KIRC cohort. (C) Nomogram prediction for 1-, 2-, 3- and 5-year overall survival of patients with KIRC. (D) 1-, 2-, 3- and 5-year calibration curves of the nomogram. KIRC, kidney renal clear cell carcinoma; MED, mediator complex; TCGA, The Cancer Genome Atlas; TNM, tumor-node-metastasis.

(Fig. 3C). According to the Kaplan-Meier analysis results of all patients, there was a marked difference between the low-risk and high-risk groups. Notably, the prognosis of the low-risk group was significantly better than that of the high-risk group; the median survival time of the high-risk group was 4.5 years (Fig. 3D). The area under the curve values for the 11 genes in the survival assessment model were 0.756 at 1 year, 0.725 at 3 years, and 0.74 at 5 years of OS (Fig. 3E).

Clinical prognostic value of a five-gene signature in KIRC patients. The prognostic role of MED family genes in KIRC was subsequently explored. The findings showed that the prognosis of patients with KIRC was strongly associated with MED11, MED16, MED18, MED21, MED25, MED29 and MED7 expression. As shown in the forest plots, of all the

factors, MED11 (HR=0.66164), MED16 (HR=0.7422), MED18 (HR=0.64535), MED21 (HR=0.57588), MED25 (HR=1.50571), MED29 (HR=0.53217) and MED7 (HR=0.51246) were significantly associated with the survival of patients with KIRC (Fig. 4A). Subsequently, multivariate Cox regression analysis was used to further evaluate the 11 genes and other clinical characteristics in patients with KIRC to identify the independent prognostic factors. MED16 (HR=0.57832), MED21 (HR=1.69538), MED25 (HR=2.67321), MED29 (HR=0.42428) and MED7 (HR=0.49732) were revealed to be independent risk factors for the prognosis of patients with KIRC (Fig. 4B). A nomogram was constructed with MED16, MED21, MED25, MED29 and MED7. The risk model based on MED16, MED21, MED25, MED29, and MED7 had good performance in predicting the prognosis of patients with KIRC, as indicated
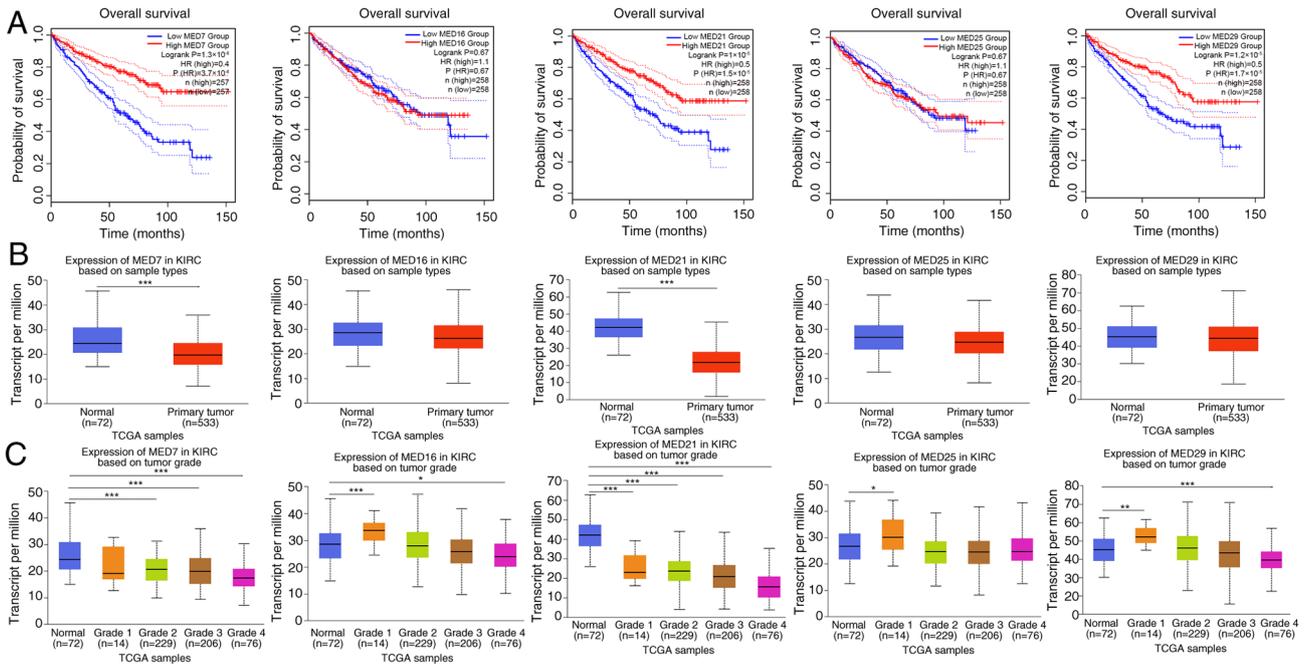
Figure 5. Prognostic feature of the mRNA expression levels of MED genes in patients with KIRC. (A) Kaplan-Meier curves of overall survival for the five MED family genes in patients with KIRC. (B) mRNA expression in patients with KIRC between tumor and normal tissues. (C) mRNA expression in patients with KIRC among different tumor grades. KIRC, kidney renal clear cell carcinoma; MED, mediator complex; TCGA, The Cancer Genome Atlas. *P<0.05, **P<0.01, ***P<0.001.

by the C-index of this model, which was 0.717 (Fig. 4C). The anticipated survival rate was close to the actual survival rate according to the 1-, 2-, 3- and 5-year nomograms (Fig. 4D). These results indicated that the five-gene signature comprising MED16, MED21, MED25, MED29 and MED7 may be useful for predicting the development of KIRC.

Prognostic features of mRNA expression. KIRC with high transcription levels of MED7, MED21 and MED29 was evidently related to a longer OS time, whereas MED16 and MED25 were not significantly associated with OS (Fig. 5A). Additionally, variations in the expression levels of MED7, MED16, MED21, MED25 and MED29 were assessed in KIRC tumor tissues (n=533) and adjacent normal tissues (n=72). Since data for adjacent normal tissues were not available for some patients, the number is unequal. The findings revealed that the expression levels of MED7 and MED21 were higher in normal tissues than in KIRC tumor tissues (Fig. 5B). Furthermore, the expression levels of MED7, MED16, MED21, MED25 and MED29 were compared between normal tissues and different KIRC tumor grade tissues. Compared with in normal tissues, the expression levels of MED7 in grade 2, grade 3 and grade 4 KIRC tissues were significantly lower. The expression level of MED16 in grade 1 tissues was higher and that in grade 4 KIRC tumor tissues was lower compared with that in normal tissues. As for MED21 expression levels, tissues from all four tumor stages, including grade 1, grade 2, grade 3 and grade 4, exhibited lower expression compared with the normal control tissues. The expression levels of MED25 in grade 1 KIRC tumor tissues were significantly higher compared with those in normal tissues. In addition, the expression level of MED29 in grade 1 tissues was higher and that in grade 4 KIRC

tumor tissues was significantly lower compared with those in normal tissues (Fig. 5C).

Relationships between MED genes and tumor-infiltrating immune cells in KIRC. The occurrence, development and metastasis of cancer are closely associated with infiltrating immune cells (21). Using the TIMER database, the potential associations between the infiltration levels of distinct immune cells and the five MED genes were explored. First, MED7 expression was strongly correlated with the infiltration of both CD8+ T cells and CD4+ T cells in patients with KIRC (Fig. 6A). The expression of MED16 was not correlated with the infiltration of CD4+ T cells, B cells and macrophages (Fig. 6B). There was also a link between MED21 expression and the infiltration of CD8+ T cells and CD4+ T cells (Fig. 6C). Additionally, the expression levels of MED25 and MED29 were not correlated with infiltrating immune cells (Fig. 6D and E).

Verification of the relationship between two MED genes and KIRC using IHC. To verify the relationship between MED genes and KIRC, MED7 and MED21 were further examined. First, IHC was performed to detect MED7 and MED21 protein expression in KIRC tissues and paired adjacent normal tissues. The clinicopathological information of the patients, including sex, age, pathological grading, pathological region and TNM stage are listed in Fig. 7A. According to the staining results, both MED7 and MED21 were more highly expressed in adjacent normal tissues than in KIRC cancer tissues (Fig. 7B).

Verification of the relationship between two MED genes and KIRC using siRNA transfection. Subsequently, corresponding siRNAs to interrupt MED7 and MED21 gene expression
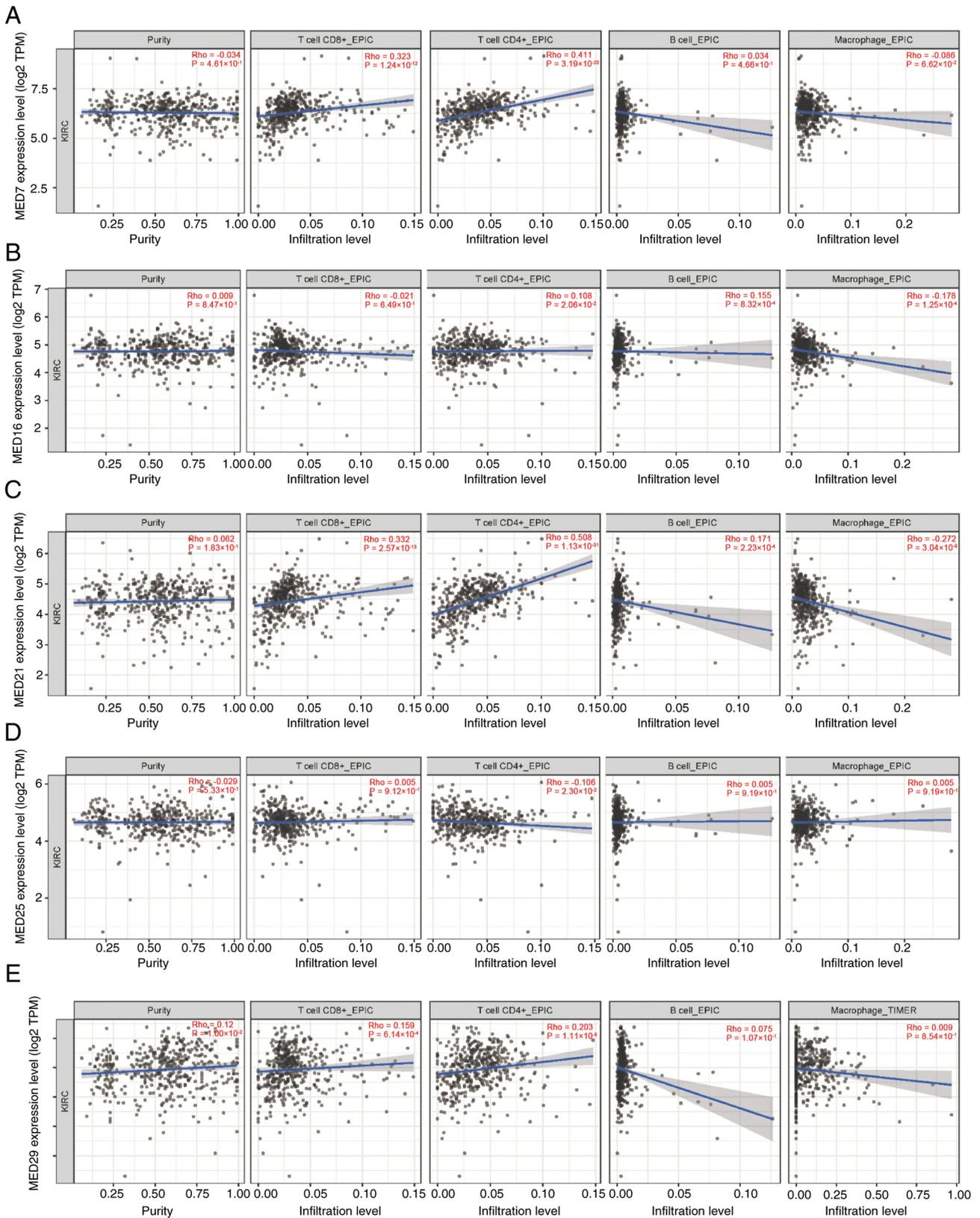
Figure 6. Relationships between MED genes and tumor-infiltrating immune cells in kidney renal clear cell carcinoma. (A) MED7. (B) MED16. (C) MED21. (D) MED25. (E) MED29. MED, mediator complex.

were designed and their effects were observed. To assess the siRNA transfection efficiency, RT-qPCR experiments were performed. All transfection efficiencies were >70% (Fig. 8A). Moreover, Transwell and wound healing assays were used to explore the association between MED7 and MED21, and cell migration in KIRC. The results revealed that MED7 and MED21 knockdown increased the migration of KIRC cells *in vitro* (Fig. 8B and C).

A

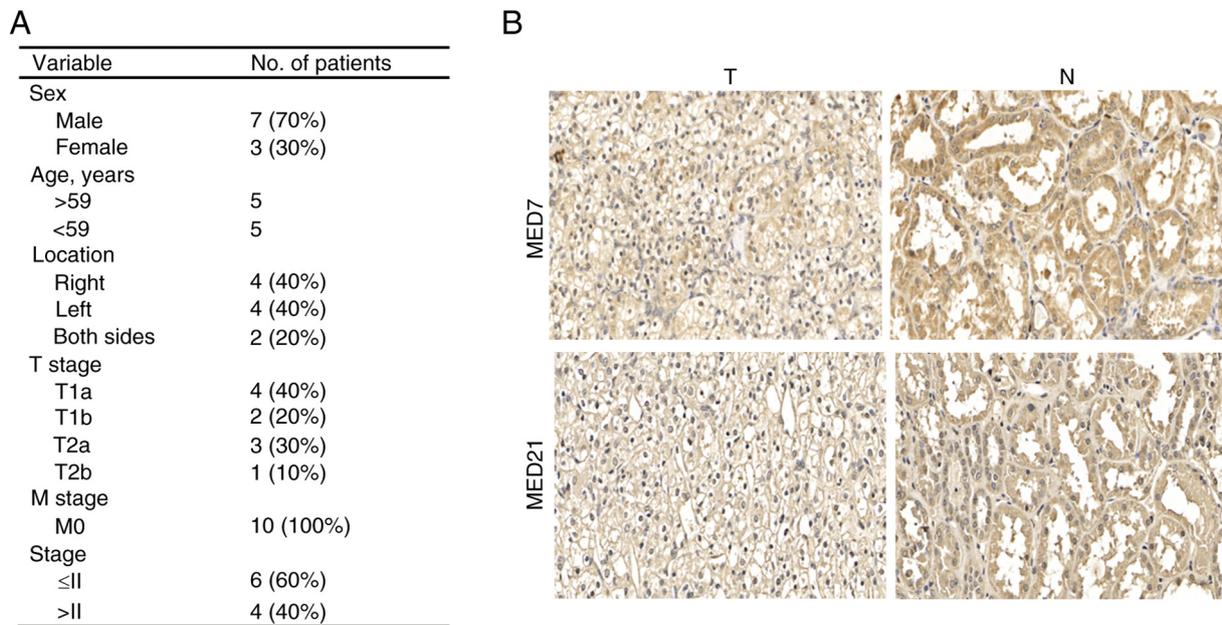| Variable	No. of patients
Sex	
Male	7 (70%)
Female	3 (30%)
Age, years	
>59	5
<59	5
Location	
Right	4 (40%)
Left	4 (40%)
Both sides	2 (20%)
T stage	
T1a	4 (40%)
T1b	2 (20%)
T2a	3 (30%)
T2b	1 (10%)
M stage	
M0	10 (100%)
Stage	
≤II	6 (60%)
>II	4 (40%)

Figure 7. Verification of the relationship between two MED genes and KIRC by immunohistochemistry analysis. (A) Clinicopathological information of 10 patients with KIRC. N and T kidney tissue was obtained from all 10 patients. (B) Expression levels of MED7 and MED21 in N and T kidney tissue (magnification, x40). KIRC, kidney renal clear cell carcinoma; MED, mediator complex; N, normal; T, tumor.

Discussion

Renal cell carcinoma is a diverse category of malignancies with various genetic and molecular changes underpinning several described histological subtypes, and it is one of the top 10 types of cancer with a rapidly increasing prevalence (22,23). Traditional chemotherapy and radiation therapy are ineffective in the treatment of kidney cancer, and immunotherapy has replaced nonspecific immunological treatments in some cases (24,25). Cancer exists in a dynamic and complex environment, the components of which change during different stages of cancer. The tumor microenvironment (TME) may affect the evolution of cancer, and there are currently several medicines, such as ipilimumab, that specifically target the TME (26,27). The MED family typically serves a key role as a regulatory element in the progression of numerous types of cancer; for example, a previous study showed that MED19 knockdown strongly hinders cell proliferation, colony-forming ability and migration *in vitro*, and downregulating MED19 can decrease the expression of cyclin D1/cyclin B1 (28). In addition, some preclinical studies have shown that MED12 is associated with DNA damage repair and TGF-β receptor signaling (29). Immune checkpoint inhibitors have been shown to significantly increase survival in various types of cancer, and another study revealed that MED12 mutation has the potential to be a predictive biomarker for immune checkpoint inhibitors in a variety of malignancies (30). Due to the immune regulatory potential of the MED family, bioinformatics analysis was used in the present study to explore the prognostic value of MED genes in KIRC.

The present study identified the most significant prognostic genes among the MED family using LASSO regression analysis; 11 genes were selected. In addition, a prognostic signature of the 11 genes was created, which performed well in prognostic predictions for patients with KIRC. In addition, the risk scores of patients with KIRC were computed and it was revealed that patients with higher MED25 levels were in the high-risk group, whereas patients with higher MED7 and MED21 expression were in the low-risk group.

In addition, univariate and multivariate Cox regression analyses were performed on the 11 genes in TCGA-KIRC cohort. The findings showed that MED16, MED21, MED25, MED29 and MED7 were independent risk factors for the prognosis of patients with KIRC and were strongly associated with survival. These findings suggested that the five MED genes may serve crucial roles in the carcinogenesis and development of KIRC.

Notably, the present study revealed that higher MED7, MED21 and MED29 transcript levels were closely related to a longer OS time in patients with KIRC. Furthermore, a nomogram was constructed based on MED16, MED21, MED25, MED29 and MED7. The calibration map revealed that the current model performed well in predicting the prognosis of patients with KIRC.

It has been demonstrated that immune infiltrates, which are a significant factor of the TME, influence tumor development and immunotherapy responses (31). Therefore, the present study analyzed the relationships between MED genes and tumor-infiltrating immune cells in patients with KIRC. The results showed that MED7 and MED21 were correlated with CD8$^+$ T cells and CD4$^+$ T cells. In addition, to further verify the relationship between MED genes and KIRC, cells in which MED7 and MED21 were knocked down were subjected to IHC, Transwell and wound healing assays due to their high expression levels in the high OS group and normal kidney tissues. The binding of human MED to RNA polymerase II is dependent on the integrity of a preserved 'hinge' in the intermediate module of the MED21-MED7 heterodimer (32). MED7 is a highly conserved subunit, and loss of MED7 has been shown to significantly affect cellular
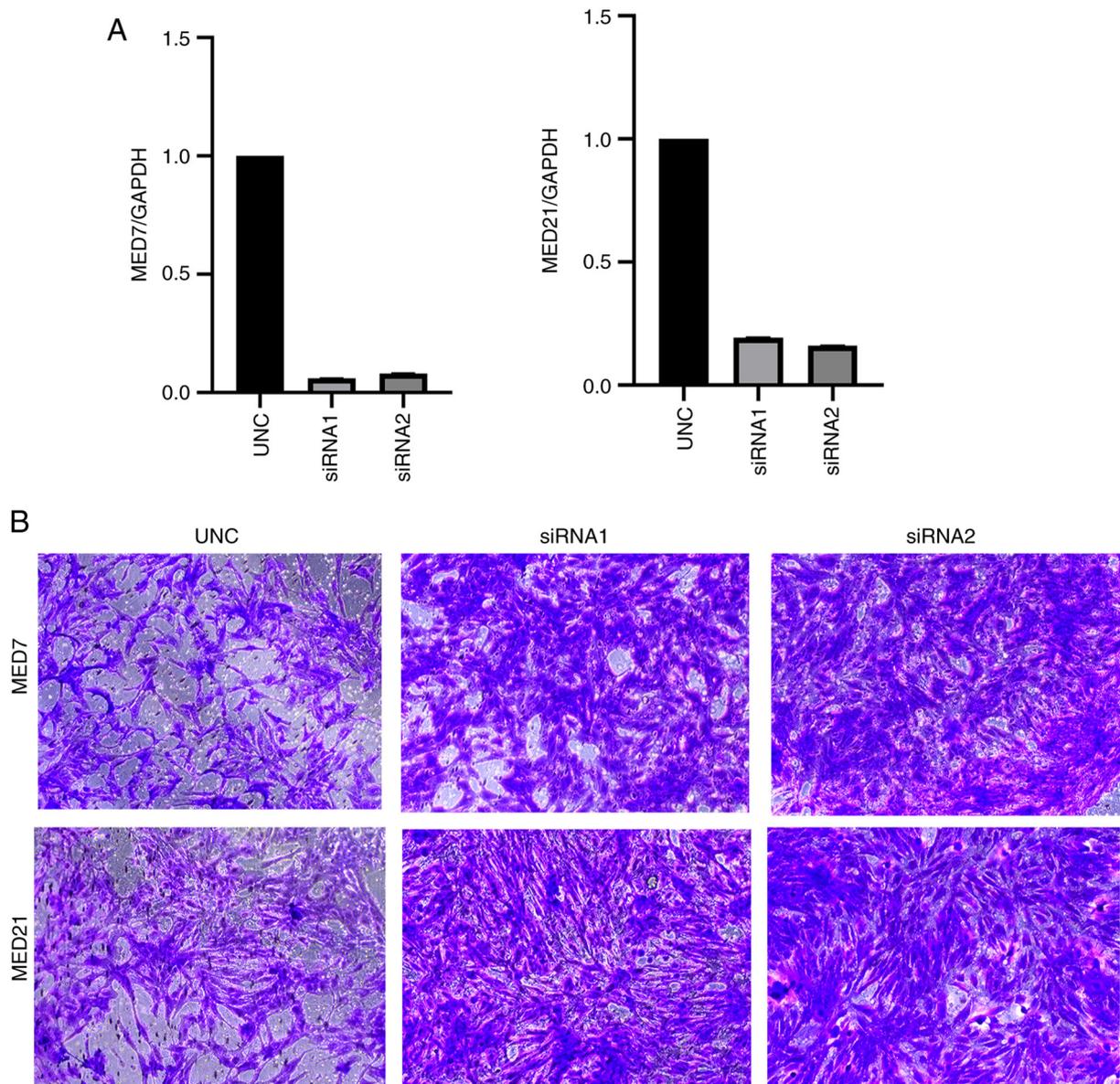
Figure 8. Continued.

functioning, including metabolic activity (12). As the most conserved MED subunit, MED21 is essential to the viability of cells in yeast and mice, and it can impact PPARA-related gene expression and metabolism (11). Furthermore, as several studies have demonstrated, MED7 and MED21 are associated with HCC (17,18). However, to the best of our knowledge, there is no research on the role of MED7 and MED21 in KIRC or other types of kidney cancer. According to the present study, the expression levels of MED7 and MED21 were greater in normal tissues than in KIRC tumor tissues. In addition, when MED7 and MED21 were knocked down, the migration of KIRC cells was increased *in vitro*.

In conclusion, a thorough analysis of the expression and prognostic significance of the MED gene family was conducted in KIRC. The results revealed that MED7, MED8, MED10, MED11, MED12L, MED15, MED16, MED18, MED21, MED25 and MED29 may serve a potential prognostic role in KIRC, and among the 11 MED genes, MED16, MED21, MED25, MED29 and MED7 were shown to be closely related to the prognosis of KIRC. These findings may aid in the improvement of the survival and prognosis of patients with KIRC.

However, there are some limitations in the present study. Firstly, since not all of the information from TCGA was available for all of the data parameters, the number of patients and controls is not totally equivalent. Secondly, the IHC results cannot determine the relationship between target antigens and survival prognosis, they can only verify the protein expression levels of target antigens between KIRC cancer tissues and paired adjacent normal tissues, due to the lack of some information about patients, such as overall survival. Thirdly, immune cell immunofluorescence staining was not performed because it was difficult to obtain the target KIRC tissues at our hospital (West China Second University Hospital, Chengdu, China), since this is a children and women's hospital.
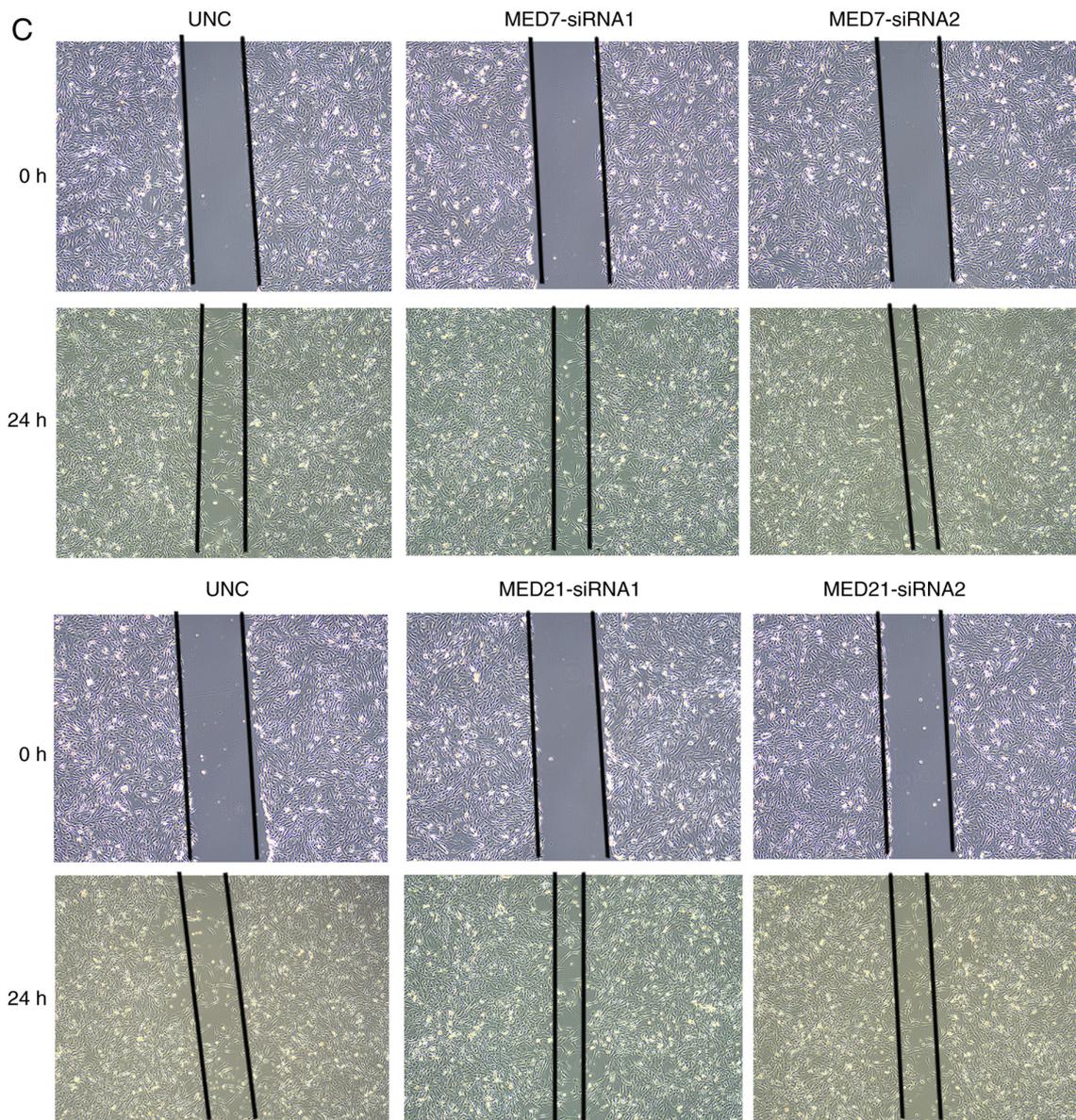
Figure 8. Verification of the relationship between two MED genes and kidney renal clear cell carcinoma by siRNA-induced knockdown. (A) Reverse transcription-quantitative PCR was used to verify the knockdown efficiency. The data are presented as the mean ± SD. (B) Migration of 786-o cells with MED7 and MED21 knockdown was assessed using an uncoated Transwell assay (48 h) (magnification, x20). (C) Migration of 786-o cells after MED7 and MED21 knockdown was measured using a wound healing assay (24 h) (magnification, x10). MED, mediator complex; UNC, universal negative control; siRNA, small interfering RNA.

Availability of data and materials

The data generated in the present study may be requested from the corresponding author.

Authors' contributions

XL and JM designed and supervised the implementation of the entire study. JM analyzed the data and completed the immunohistochemistry experiment. MW completed the Transwell and wound healing assays, and wrote the manuscript. MM analyzed the data and organized the images. XL and JM confirm the authenticity of all the raw data. All authors read and approved the final version of the manuscript.

Ethics approval and consent to participate

The study was approved by the Institutional Review Board of West China Second University Hospital (ethics approval no. 2023-012). All of the datasets were retrieved from

the online databases; therefore, it was confirmed that written informed consent had already been obtained, which was also the case for the purchased tissue microarray.

Patient consent for publication

Not applicable.

Competing interests

The authors declare that they have no competing interests.

References

1. Owens B: Kidney cancer. Nature 537: S97, 2016.
2. Linehan WM, Schmidt LS, Crooks DR, Wei D, Srinivasan R, Lang M and Ricketts CJ: The metabolic basis of kidney cancer. Cancer Discov 9: 1006-1021, 2019.
3. Ricketts CJ, De Cubas AA, Fan H, Smith CC, Lang M, Reznik E, Bowlby R, Gibb EA, Akbani R, Beroukhim R, *et al*: The cancer genome atlas comprehensive molecular characterization of renal cell carcinoma. Cell Rep 23: 313-326.e315, 2018.
4. Turajlic S, Swanton C and Boshoff C: Kidney cancer: The next decade. J Exp Med 215: 2477-2479, 2018.
5. Latif F, Tory K, Gnarra J, Yao M, Duh FM, Orcutt ML, Stackhouse T, Kuzmin I, Modi W and Geil L: Identification of the von Hippel-Lindau disease tumor suppressor gene. Science 260: 1317-1320, 1993.
6. Zhang Y, Qin P, Tian L, Yan J and Zhou Y: The role of mediator complex subunit 19 in human diseases. Exp Biol Med (Maywood) 246: 1681-1687, 2021.
7. Napoli C, Schiano C and Soricelli A: Increasing evidence of pathogenic role of the mediator (MED) complex in the development of cardiovascular diseases. Biochimie 165: 1-8, 2019.
8. Chadick JZ and Asturias FJ: Structure of eukaryotic Mediator complexes. Trends Biochem Sci 30: 264-271, 2005.
9. Singh N and Han M: sur-2, a novel gene, functions late in the let-60 ras-mediated signaling pathway during Caenorhabditis elegans vulval induction. Gene Dev 9: 2251-2265, 1995.
10. Grants JM, Goh GY and Taubert S: The mediator complex of caenorhabditis elegans: Insights into the developmental and physiological roles of a conserved transcriptional coregulator. Nucl Acids Res 43: 2442-2453, 2015.
11. Bourbon HM: Comparative genomics supports a deep evolutionary origin for the large, four-module transcriptional mediator complex. Nucleic Acids Res 36: 3993-4008, 2008.
12. Koschubs T, Seizl M, Larivière L, Kurth F, Baumli S, Martin DE and Cramer P: Identification, structure, and functional requirement of the Mediator submodule Med7N/31. EMBO J 28: 69-80, 2009.
13. Zhang X, Gao D, Fang K, Guo Z and Li L: Med19 is targeted by miR-101-3p/miR-422a and promotes breast cancer progression by regulating the EGFR/MEK/ERK signaling pathway. Cancer Lett 444: 105-115, 2019.
14. Mehine M, Mäkinen N, Heinonen HR, Aaltonen LA and Vahteristo P: Genomics of uterine leiomyomas: Insights from high-throughput sequencing. Fertil Steril 102: 621-629, 2014.
15. Zhu LJ, Yan WX, Chen ZW, Chen Y, Chen D, Zhang TH and Liao GQ: Disruption of mediator complex subunit 19 (Med19) inhibits cell growth and migration in tongue cancer. World J Surg Oncol 11: 116, 2013.
16. Joseph C, Macnamara O, Craze M, Russell R, Provenzano E, Nolan CC, Diez-Rodriguez M, Sonbul SN, Aleskandarany MA, Green AR, *et al*: Mediator complex (MED) 7: A biomarker associated with good prognosis in invasive breast cancer, especially ER+ luminal subtypes. Br J Cancer 118: 1142-1151, 2018.
17. Chen ZL, Ma YY, Mou XZ and Zhang JG: Upregulation of MED7 was associated with progression in hepatocellular carcinoma. Cancer Biomark 38: 603-611, 2023.
18. Tan W, Peng S, Li Z, Zhang R, Xiao Y, Chen X, Zhu J, Li B and Lv X: Identification of therapeutic targets and prognostic biomarkers among genes from the mediator complex family in the hepatocellular carcinoma tumour-immune microenvironment. Comput Math Methods Med 2022: 2021613, 2022.
19. Sato S, Tomomori-Sato C, Tsai KL, Yu X, Sardiu M, Saraf A, Washburn MP, Florens L, Asturias FJ, Conaway RC and Conaway JW: Role for the MED21-MED7 hinge in assembly of the mediator-RNA polymerase II holoenzyme. J Biol Chem 291: 26886-26898, 2016.
20. Livak KJ and Schmittgen TD: Analysis of relative gene expression data using real-time quantitative PCR and the 2(-Delta Delta C(T)) method. Methods 25: 402-408, 2001.
21. Steven A and Seliger B: The role of immune escape and immune cell infiltration in breast cancer. Breast care (Basel) 13: 16-21, 2018.
22. Siegel RL, Miller KD and Jemal A: Cancer statistics, 2018. CA Cancer J Clin 68: 7-30, 2018.
23. Shuch B, Amin A, Armstrong AJ, Eble JN, Ficarra V, Lopez-Beltran A, Martignoni G, Rini BI and Kutikov A: Understanding pathologic variants of renal cell carcinoma: Distilling therapeutic opportunities from biologic complexity. Eur Urol 67: 85-97, 2015.
24. Goyal R, Gersbach E, Yang XJ and Rohan SM: Differential diagnosis of renal tumors with clear cytoplasm: Clinical relevance of renal tumor subclassification in the era of targeted therapies and personalized medicine. Arch Pathol and Lab Med 137: 467-480, 2013.
25. Choueiri TK and Motzer RJ: Systemic therapy for metastatic renal-cell carcinoma. N Eng J Med 376: 354-366, 2017.
26. Quail DF and Joyce JA: Microenvironmental regulation of tumor progression and metastasis. Nat Med 19: 1423-1437, 2013.
27. Coussens LM, Zitvogel L and Palucka AK: Neutralizing tumor-promoting chronic inflammation: A magic bullet? Science 339: 286-291, 2013.
28. Yu W, Zhang Z, Min D, Yang Q, Du X, Tang L, Lin F, Sun Y, Zhao H, Zheng S, *et al*: Mediator of RNA polymerase II transcription subunit 19 promotes osteosarcoma growth and metastasis and associates with prognosis. Eur J Cancer 50: 1125-1136, 2014.
29. Huang S, Hölzel M, Knijnenburg T, Schlicker A, Roepman P, McDermott U, Garnett M, Grernrum W, Sun C, Prahallad A, *et al*: MED12 controls the response to multiple cancer drugs through regulation of TGF-β receptor signaling. Cell 151: 937-950, 2012.
30. Zhou Y, Tan Y, Zhang Q, Duan Q and Chen J: MED12 mutation as a potential predictive biomarker for immune checkpoint inhibitors in pan-cancer. Eur J Med Re 27: 225, 2022.
31. Zhang Y and Zhang Z: The history and advances in cancer immunotherapy: Understanding the characteristics of tumor-infiltrating immune cells and their therapeutic implications. Cell Mol Immunol 17: 807-821, 2020.
32. Robinson PJ, Trnka MJ, Pellarin R, Greenberg CH, Bushnell DA, Davis R, Burlingame AL, Sali A and Kornberg RD: Molecular architecture of the yeast mediator complex. eLife 4: e08719, 2015.